Statnamic testing of model piles in a clay calibration chamber

Brown, Michael; Anderson, William; Hyde, Adrian

Published in:
International Journal of Physical Modelling in Geotechnics

DOI:
10.1680/ijpmg.2004.4.1.11

Publication date:
2004

Document Version
Publisher's PDF, also known as Version of record

IJPMG-International Journal of Physical Modelling in Geotechnics 1 (2004) : 11-24

STATNAMIC TESTING OF MODEL PILES IN A CLAY CALIBRATION CHAMBER

MICHAEL BROWN[i], WILLIAM ANDERSON[ii] AND ADRIAN HYDE[iii]

ABSTRACT

The rate of load application during a Statnamic pile test lies between that for static and dynamic pile tests. Current analysis methods offer excellent correlation between Statnamic and static test results for coarse-grained soils. However, over-prediction of pile load capacity can be obtained for fine-grained soils. It is very difficult to explore this anomaly using full scale field tests because of natural soil variability, so a study has been carried out using a model pile installed in similar clay beds prepared in a large triaxial calibration chamber. The instrumented model pile has been loaded at varying rates by a computer controlled servo-hydraulic actuator. The tests have simulated static loading, constant rate of penetration at various rates of penetration, and Statnamic loading. Results suggest that components of the rate effect associated with increased pile penetration rates may be described by a power law relationship.

Key words: pile, clay, static loading, damping, calibration chamber, 1-g model

INTRODUCTION

The Statnamic test was developed in the late 1980s to try to overcome some of the problems associated with conventional static and dynamic pile load tests (Middendorp, 1993). Static pile tests are very expensive because of the reaction load required. Dynamic tests do not require this reaction but empirical corrections have to be made for energy losses and the rapid application of load can cause complex wave interactions making results very difficult to interpret.

Statnamic testing works by the rapid burning of fuel that produces gas in a pressure chamber (Fig. 1). The venting of this gas accelerates a mass upward that in turn imparts a load onto a pile. The load is applied and removed by the controlled venting of the gas which results in a load application of ≈ 180 ms which is 30 times that of dynamic loading (Bermingham et al., 1994).

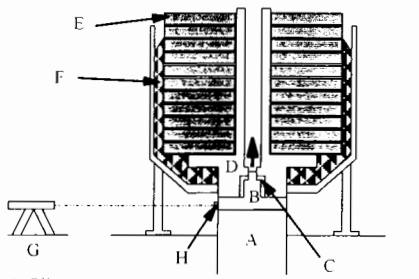

Fig. 1. Key features of Statnamic testing

For foundation design it is necessary to derive the equivalent static load-displacement curve from the Statnamic data. The simplest form of analysis used to obtain equivalent static pile response is known as the unloading point method (UPM) (Kusakabe and Matsumoto, 1995). In this method of analysis, the pile and soil are modeled as a single mass (M) supported by a spring (stiffness, K) and dashpot (damping coefficient, C) in parallel as shown in Fig. 2. The spring is used to represent the force-displacement behaviour under static loading (F_u) and the dashpot (damper) represents velocity dependent viscous soil resistance (F_v). The UPM works by determining a constant damping coefficient that when multiplied by the velocity gives the viscous soil resistance that may be subtracted from the Statnamic load to obtain the static load. In this method, the magnitude of the damping coefficient is obtained by first determining the static soil resistance at the unloading point, F_{unl} in Fig. 2, where although the pile's inertia is non-zero, the pile velocity and hence damping are zero. This same static soil resistance together with the inertia is then subtracted from the maximum Statnamic load, $F_{STN(max)}$, to determine the viscous component of resistance.

The Statnamic analysis method was conceived to be simple and based on the measured results alone. This was to avoid the criticisms of dynamic analysis being heavily dependant on user selected empirical parameters. However, the analysis method makes several assumptions that may significantly influence the accuracy of predictions. These include assuming that the pile is a rigid body, that

i) Research Associate, Department of Civil and Structural Engineering, University of Sheffield, Mappin Street, Sheffield, S1 3JD, UK.
ii) Professor, ditto.
iii) Reader, ditto.
Manuscript was received for review on August 18, 2003.

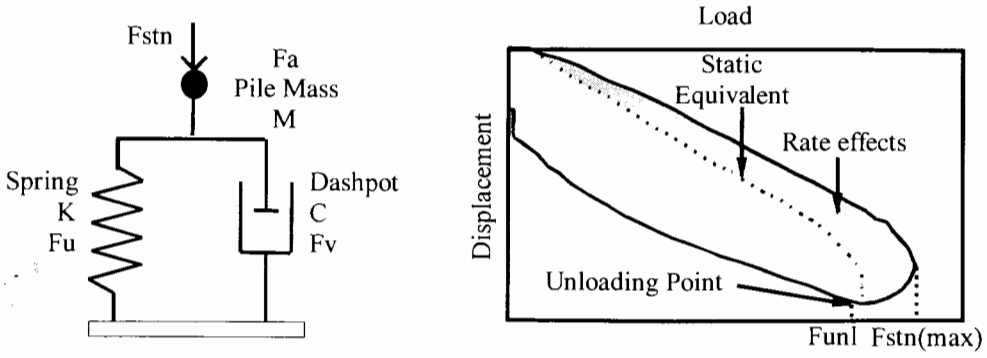

Fig. 2. Rheology and interpretation of Statnamic test data

the damping model is linear (i.e. C is a constant), that the soil is elastic - perfectly plastic, and that inertial effects are limited to the pile. In addition, the effects of excess pore water pressure generation and dissipation during and after loading are ignored.

Although the present analysis has shortcomings it generally provides excellent correlation with static tests for sands and gravels (Brown, 1994), but may over-predict pile capacities by up to 30% for fine grained soils (clays). This is thought to be due to strain rate dependency of clay's shear strength and stiffness. For clay, shear strength and stiffness increase significantly with increasing rate of deformation (Casagrande and Shannon, 1948). Unfortunately, the rate effect or damping coefficient for clays is highly non-linear resulting in the over-predictions mentioned above and a reluctance to adopt the Statnamic test method for piles in clay. However, a study by Hyde et al. (1998) suggested that if the rate effects could be expressed as a power law for non-linear damping, it should be possible to get a better estimate of the static resistance of piles in clay from Statnamic tests. The commercial advantages of being able to use Statnamic testing in countries such as the UK, which has large areas covered by normally and overconsolidated clay deposits, would be considerable. A programme of research has therefore been initiated to investigate Statnamic testing of piles in clay deposits.

MODEL TESTING

Present understanding of the Statnamic test and the analysis of the test results are predominantly based upon comparative field studies. These are normally part of routine pile foundation installation and testing, and lack the quality of site investigation and instrumentation that are necessary for rigorous research purposes. Even if the highest quality field study, which would be very expensive, were carried out, the results would inevitably be influenced by natural soil variation.

These limitations may be overcome by carrying out tests on instrumented model piles installed in beds of clay prepared with known stress history and subject to known boundary conditions. The inclusion of instrumentation in the beds allows certain aspects of the Statnamic test to be examined in more detail than would be possible in the field.

The use of a 1-g model test, compared with centrifuge model tests, has the advantages of relatively low cost, simpler scaling laws and the ability to investigate testing events associated with high accelerations. The accelerations may cause particular problems when attempting to carefully control the movement of bodies through the non-linear acceleration field associated with a centrifuge test (Bell, 1987). However, there are limitations to using clay beds for 1-g models testing. Clay bed preparation by consolidating a slurry may take some considerable time and there are limited vertical stress variations associated with a relatively small bed at 1-g (Taylor, 1995). The model in this study only considers pile tip behaviour and adjacent skin friction resistance of a pile section installed at some depth equivalent to the applied effective vertical stress, so the latter was not considered a major shortcoming.

To replicate field conditions in a soil bed in the laboratory for studies of any penetrating or embedded object it is necessary to minimise the boundary influence. This can be done by having a clay bed that is sufficiently large that any rigid boundary does not affect behaviour, or by using boundaries that can be stress controlled.

Using undrained cavity expansion theory, and assuming elastic-perfectly plastic soil behaviour, Smith (1993) calculated that the diameter of any clay test chamber with a rigid boundary should be at least 20 times the diameter of the test object. Eid (1978) carried out model pressuremeter tests in clay beds prepared in a rigid body calibration chamber with a diameter 40 times that of the model pressuremeter. She found that at a pressuremeter radial expansion of less than 4% the rigid boundary began to have a significant effect. A rigid boundary test chamber for testing model piles of any reasonable dimensions would therefore have to be of the order of metres in diameter, thus creating space and preparation problems. A further complication with dynamic loading in a rigid

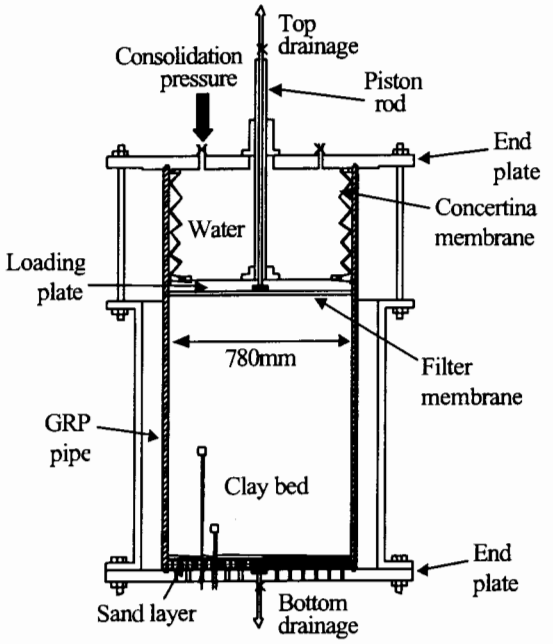

Fig. 3. One-dimensional consolidation of clay slurry in the consolidometer

body container is the reflection of stress waves from the boundary.

With a flexible stress controlled boundary a much smaller clay bed may be used. Using Smith's approach it can be shown that a bed with a minimum diameter of 5 to 6 times that of the model pile should be adequate to simulate a semi-infinite soil mass.

The clay calibration chamber

The clay calibration chamber adapted for this study was originally designed to produce clay beds from slurry for full scale tests using the self boring pressuremeter (Anderson et al., 1991). The clay bed was prepared in two stages prior to model pile testing, i.e. one-dimensional (K_o) consolidation in a consolidometer (Fig. 3) followed by isotropic consolidation in a triaxial chamber (Fig. 4).

During the preparation of a large clay bed the slurry undergoes considerable volume change due to consolidation. To accommodate this volume change, a 1.7 m high glass reinforced plastic pipe (785 mm internal diameter, 23 mm wall thickness) was used for initial one-dimensional consolidation. The pipe was clamped between the chamber top and bottom end plates to form the consolidometer.

The clay slurry was subjected to a vertical consolidation stress by pressurising a water filled concertina membrane clamped to a 20 mm thick steel loading plate (Fig. 3). To guide the movement of the loading plate during consolidation, a 50 mm diameter hollow piston rod, passing through an O-ring sealed bush bolted to the top end plate, was connected to the loading plate. A displacement transducer resting on the piston rod allowed measurement of the bed's settlement during consolidation. The concertina membrane and piston arrangement were designed to accommodate up to 700 mm settlement during one-dimensional consolidation.

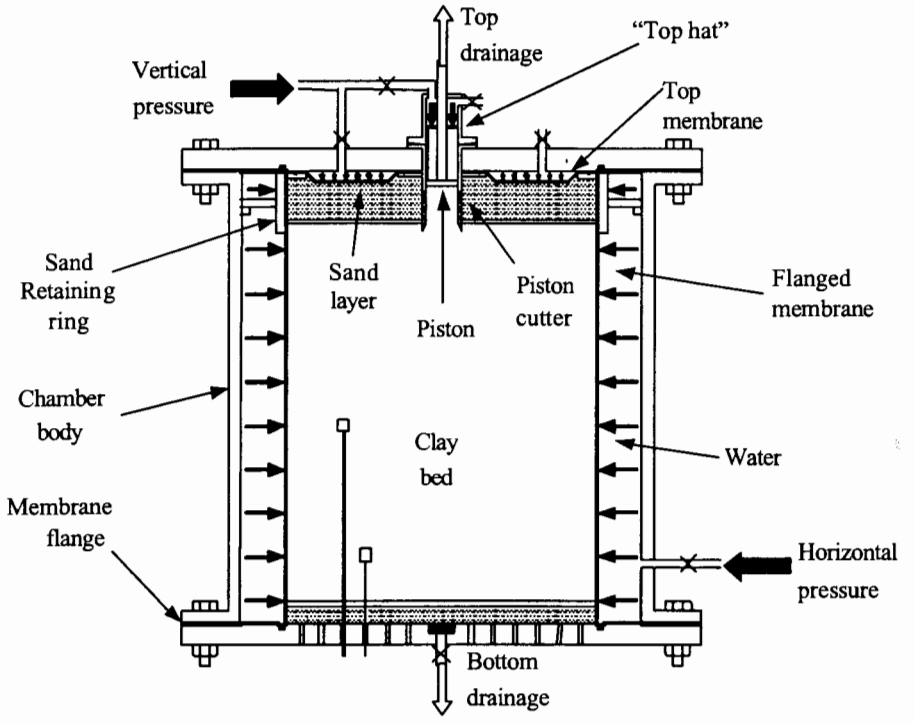

Fig. 4. Triaxial consolidation in the clay calibration chamber

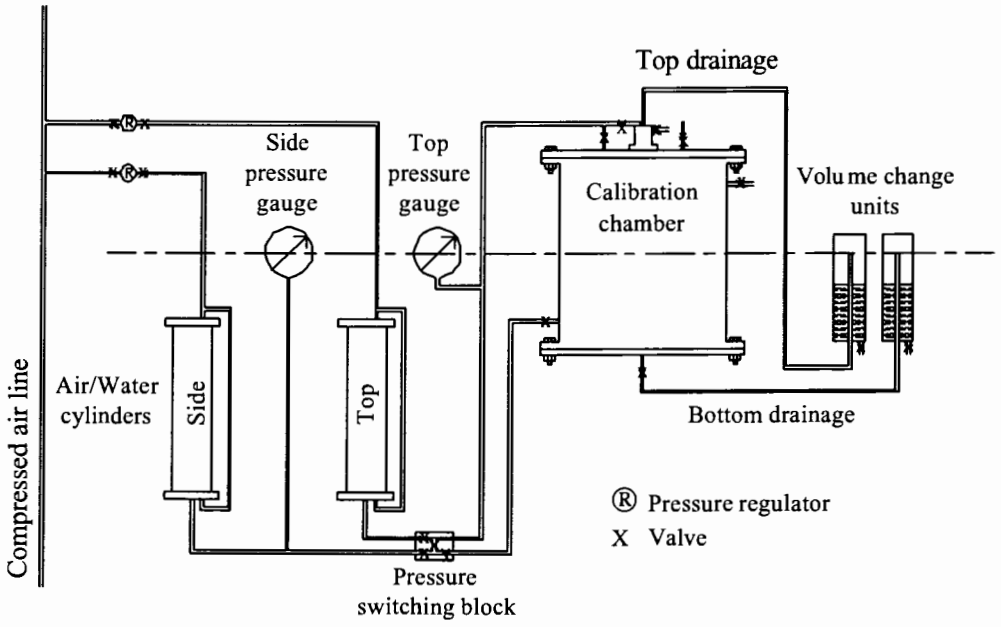

Fig. 5. Pressure and drainage arrangements for the calibration chamber

The design of the consolidometer allowed for pore water drainage from both the top and the bottom of the clay bed throughout all stages of bed preparation and subsequent testing. At the top of the bed there was a 2 mm thick plastic filter membrane, with an average pore size of 30 μm, through which water could drain via the hollow piston rod to the top volume change unit (Fig. 5). The clay bed was separated from the base end plate by a similar layer of porous plastic underlain by a 15 to 20 mm thick sand layer allowing pore water drainage to the bottom volume change unit.

There were nineteen 7 mm diameter holes in the base end plate to allow instrumentation to be incorporated in the clay bed (Figs. 3 & 4). Using these holes transducers could be positioned at various heights and radial distances from the model pile. To maintain the position of the transducers during consolidation, they were mounted on greased hollow thin walled metal tubes clamped through the base end plate holes.

The second stage of the consolidation process was isotropic consolidation in the triaxial chamber shown in Fig. 4. The outer chamber body consisted of a 1,030 mm outer diameter steel pipe, 13 mm thick with reinforced flanges at each end. A flanged rubber membrane was placed around the clay bed in a similar manner to the membrane in a conventional triaxial test. The flanges of the membrane were clamped between the outer calibration chamber body and the top and bottom end plates. Horizontal confining stress was applied to the clay bed by pressurising the water surrounding it.

During triaxial consolidation the vertical stress was applied to the clay bed by water pressure acting through a rubber membrane clamped to the top end plate. This upper membrane was designed to accommodate bed settlements of up to 100 mm. To allow for the slight difference in the height of each bed at the end of one-dimensional consolidation, a sand layer was placed on top of the bed, separated from it by a porous plastic filter. The sand layer transferred pressure to the clay bed, as well as acting as a drainage path. During cell assembly, a retaining ring was placed around the top of the outside rubber membrane to retain this sand layer.

The top end plate had a 100 mm diameter hole at its centre through which the test devices or models could be inserted into the clay bed. During the one-dimensional consolidation the piston rod passed through this hole (Fig. 3), but during the triaxial consolidation a piston cutter was fitted into it (Fig. 4). A piston fitted with a rolling Bellofram seal ran inside the piston cutter and was enclosed by a "top hat" that allowed the application of uniform vertical stress to the bed in this area and provided a top drainage outlet.

To apply pressure to the chamber during both K_0 consolidation and triaxial consolidation, the chamber was connected to two identical air/water systems fitted with valves to regulate the compressed air pressure (Fig. 5). During the initial one-dimensional consolidation stage, the two systems were linked together to supply sufficient water to accommodate the large consolidation volume changes that were likely to occur. For triaxial consolidation, a pressure-switching block separated the systems and individual regulators controlled the top and radial pressures. This system may be used to subject the bed to different vertical and horizontal stresses, but in this study an isotropic stress regime was used for all tests. Water expelled from the clay bed during consolidation was collected in

two separate volume change units mounted at the mid-height of the clay bed.

Clay bed material

In the previous clay calibration chamber studies (Anderson et al., 1991) powdered kaolin was used to make the clay slurry. Kaolin has the benefit of being widely available and has an extensive record of use in research, but it has a number of shortcomings that have been summarised by Rossato et al. (1992). These include having a very high clay fraction (80%) leading to particles becoming easily orientated during consolidation and shear. It also displays fully developed residual shear behaviour at strains as low as 12%, independent of sample size. This behaviour may be particularly advantageous in certain studies but may have detrimental effects in large model studies where simulations of natural soils are required. The bed material chosen for this study was therefore similar to that proposed by Rossato et al. (1992) and which consisted of a mix of kaolin, sand and silt (KSS). The components used in the KSS were chosen to be as close as possible to those proposed by Rossato et al. (1992) and were as follows:

1) Sand: Buckland P30 Silica Sand (sub-angular to sub-rounded), Lower Greensand origin (Cretaceous).
2) Silt: Oakamoor HPF4 Silica flour, high purity dry ground quartz sand (98 % min quartz content), Upper Millstone Grit origin (Carboniferous).
3) Kaolin: Speswhite very fine china clay.

The kaolin and silt were identical to Rossato et al. (1992), but the sand was of coarser grading with 45% above 300 μm rather than 10%. This resulted in a final clay content of 38% (Table 1) whereas Rossato et al. (1992) had clay content of 48%. Similar materials have been proposed by McManus & Kulhawy (1991) for 1-g model testing of piles.

The mix proportions (by weight) used to form the clay beds were 50% kaolin, 25% sand and 25% silt. Index properties for this mix are shown in Table 1 (Balderas-Meca, 2004). The clay bed was formed by consolidating thoroughly mixed KSS slurry with a moisture content of 55%, which was equivalent to 1.5 times the liquid limit, the minimum suggested by Sheeran and Krizek (1971) for the preparation of consistent slurries. Using this minimum water content instead of the more commonly used 2 times liquid limit had the benefits of shorter consolidation times for the beds and the consolidometer did not require topping up with slurry as consolidation progressed.

Clay bed preparation

Before clay bed preparation started the transducers required within the bed were placed on thin walled rods set at various heights and radial positions above the chamber base end plate. The pore pressure transducers were Druck PDCR 81 units as used by Bond et al. (1991). They found that the units had a 99 % response to step loads of ± 800 kPa within 10 to 400 ms. Additionally, the bed contained Kistler 8704B50 piezoelectric accelerometers capable of measuring vertical accelerations within the bed and for some beds a Kulite 0234 earth pressure cell with a fluid filled low deflection diaphragm to monitor vertical stress at the base of the clay bed. The pore pressure transducers were vacuum deaired and kept in their de-airing cell until chamber assembly commenced. Thereafter, to minimise the possibility of them becoming de-aired, they were smeared with KSS slurry and sealed in plastic bags. The inside wall of the consolidometer body was then smeared with silicon grease to reduce wall friction and positioned on the chamber end plate.

Slurry preparation was undertaken in a large pan mixer. The required volume of de-aired and de-ionised water (50 litres) followed by the kaolin (45.5 kg) and silt (22.75 kg) were added to the pan. This was then mixed for 5 minutes to a slurry before the sand was added gradually to avoid segregation. Mixing continued for a minimum of 30

Table 1. Index and engineering properties of the KSS material

Property	Symbol	Value
Liquid limit	LL	37%
Plastic limit	PL	17%
Plasticity index	PI	20%
Specific gravity of solids	G_s	2.64
Clay fraction (% < 2 μm)	CF	38%
Activity	A	0.53
Coefficient of vertical permeability in terms of void ratio, e (σ'_v from 50 to 500 kPa)	k_v	$6.32e^{3.31}x10^{-9}$ m/s
Slope of consolidation line	λ	0.159
Slope of swelling line	κ	0.023
Slope of critical state line	M	1.05 ($\phi' = 26.6°$)

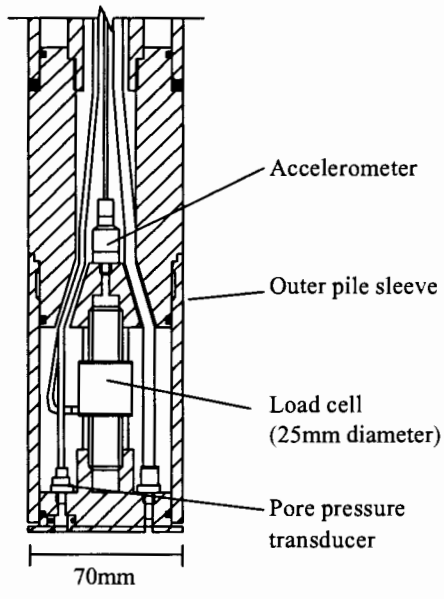

Fig. 6. Model pile tip details

minutes. The slurry was transferred to the consolidometer using a slurry pump with the slurry maintained under water to avoid air entrapment. When the rising water on top of the slurry reached the pore pressure transducers their plastic bag covers were removed. Eight mixes were required to fill the consolidometer to approximately 1.4 m above the chamber base. Once slurry addition was complete, any excess water was removed and the top drainage layer added (Fig. 3). The loading plate and concertina membrane were then lowered onto the slurry surface and the top end plate bolted in position.

Initially the vertical pressure applied to the bed was maintained at 75 kPa for 3 to 4 days. After this stage the pressure was increased to 280 kPa. Continuous system monitoring throughout this period included bed drainage volumes, piston settlement, applied pressure, bed pore water pressures and, for some beds, vertical total stress.

One-dimensional consolidation was stopped after approximately 3 weeks when the clay bed was found to be self-supporting. The termination criteria used were:

1) Clay bed height equal to or less than 1 m.
2) Average degree of consolidation, as indicated by the clay bed pore pressure transducers, greater than 40%.
3) Mid-height excess pore water pressure less than 150 kPa.

When all of these criteria were satisfied the drainage valves to the bed were closed to minimise swelling and the consolidation pressure slowly reduced to zero. The top end plate and loading plate arrangement were removed and the consolidometer jacked off the bed. The freestanding bed was then ready for conversion to triaxial mode as shown in Fig. 4. The bed was carefully fitted with the flanged rubber membrane and the chamber body bolted to the bottom end plate. The sand retaining ring was put into position below the flange of the flanged rubber membrane, and sand used to bring the height of the bed up to the required level. The top end plate and its accessories could then be fitted.

Consolidation of the bed was restarted with a 280 kPa water pressure being applied both radially and vertically. During this isotropic consolidation stage drainage occurred from both the top and the bottom of the bed, with volume change and bed pore pressure readings being recorded. An average bed consolidation of 90% was reached in less than 8 days, at which stage it was considered suitable to begin testing.

Model pile

The stainless steel model pile had total length 1295 mm and a diameter of 70 mm, giving a pile/clay bed diameter ratio of 11, i.e. well above the minimum of 5 to 6 mentioned earlier. It consisted of several sections and was designed to independently measure pile tip and skin friction loads as well as pore water pressures at the pile/soil interfaces. The major sections consisted of the pile tip, skin friction sleeve and the pile top with end plate seal.

The pile tip section incorporated an Entran load cell that was connected to the pile tip end plate that moved within the pile outer skin (Fig. 6) to measure end bearing load. A Kulite XT-123C-190 pore pressure transducer, saturated with silicon oil with a kinematic viscosity approximately 17 times that of water, was also included in the pile tip end plate.

Located above the pile tip section was the 302 mm long skin friction sleeve (Fig. 7). This section of the pile was designed to measure the skin friction resistance over a known pile length without being influenced by other components of the pile capacity. This was achieved by placing a strain gauged aluminium dumb bell load cell outside the central structural element of the pile. The central cylinder transmitted the forces resisting the pile in front of the friction sleeve. The load cell passed over this with clearance. The friction sleeve was bolted directly to the load cell without connection to the rest of the pile. To compress the load cell the skin friction sleeve was located such that the load cell was in permanent contact with the pile at its top. Located directly above the skin friction sleeve was another Kulite pore pressure transducer similar to that placed in the pile tip. The outer surface of the pile was machined in the same manner throughout to maintain consistent surface roughness (R_a = 0.64 to 0.83 μm). The pile surface was considerably smoother than that associated with prototype piles (R_a = 10 μm, Department of Energy, 1990) but no attempt was made in the study to model this although it is acknowledged that mobilised friction angles and shaft resistances would be low.

A special section was required where the pile extended through the chamber top so that a seal was maintained

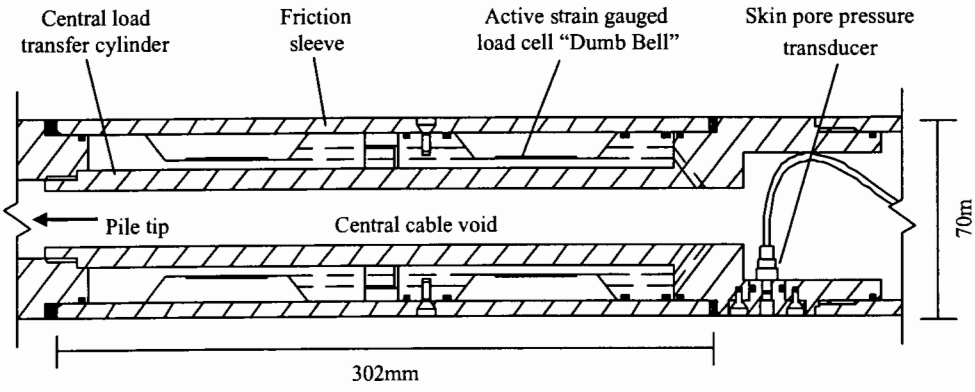

Fig. 7. Model pile skin friction sleeve details

but friction under rapid pile loading kept to a minimum. This was achieved by the use of a Bellofram type rolling diaphragm seal as shown in Fig. 8. The sealing boss for the diaphragm seal also incorporated an outlet for top drainage during consolidation after pile installation.

Model pile installation

The pile was installed during the triaxial consolidation phase. Prior to introducing the pile the top and radial pressures were slowly reduced to zero. The 'top hat' was then de-pressurised and the piston removed. The sand within the piston cutter was carefully excavated down to the porous plastic membrane and the top surface of the clay bed exposed. Pile installation proceeded by installing a thin walled casing tube through the hole in the top plate, with vertical positioning and depth control being provided by a guiding plate attached centrally at the top of the chamber.

A hole was then excavated by a 90 mm long auger lowered down the inside of the casing. Once the auger reached the end of its travel, it was removed and the casing was advanced to support the void. This process was repeated until the tip of the casing was at the final required pile tip depth. A measured volume of de-aired and de-ionised water was introduced to the base of the excavation in attempt to maintain pore pressure transducer saturation and the model pile was carefully lowered into place, air and surplus water drained out through a flushing tube within the pile. The casing was then jacked out.

Once the pile was in place the rolling Bellofram seal attached to the pile was clamped down along with the Bellofram sealing boss (Fig. 8) and the pile was held in position by a clamp. The clay bed instrumentation tubes were removed and the water pressure was gradually re-applied to the bed allowing isotropic consolidation to continue until all the indications were that the bed was at least 90% consolidated.

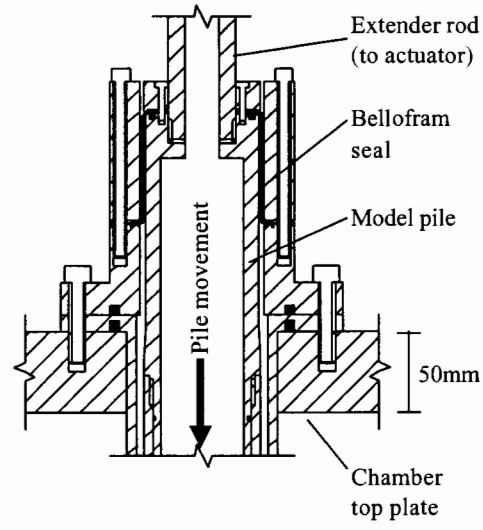

Fig. 8. Chamber top plate/pile sealing arrangement

Pile servo-hydraulic loading system

A high-speed servo-hydraulic actuator mounted rigidly above the calibration chamber (Fig. 9) was used to carry out both displacement and load controlled testing. The control and data acquisition from the loading system instrumentation was undertaken by a PC fitted with a high-speed (1.25 MHz), 64 Channel, 12-bit data acquisition card (DAQ), as shown in Fig. 10.

The system was based on an unequal area servo actuator capable of applying loads of 41.4 kN statically and 27.3 kN dynamically with a total stroke length of 150 mm. Oil flow to the actuator was provided by a mobile hydraulic power pack. To aid response of the system both the pressure and return hydraulic flow lines were fitted with accumulators. A 40 kN fatigue rated load cell at the tip of the actuator rod was located between the pile and the actuator during testing. This load cell was used to measure the total resistance of the pile as well as providing a feedback signal during load control tests. The actuator also incorporated an internal 150 mm stroke linear displacement transducer (LVDT) that was used to provide a feed-

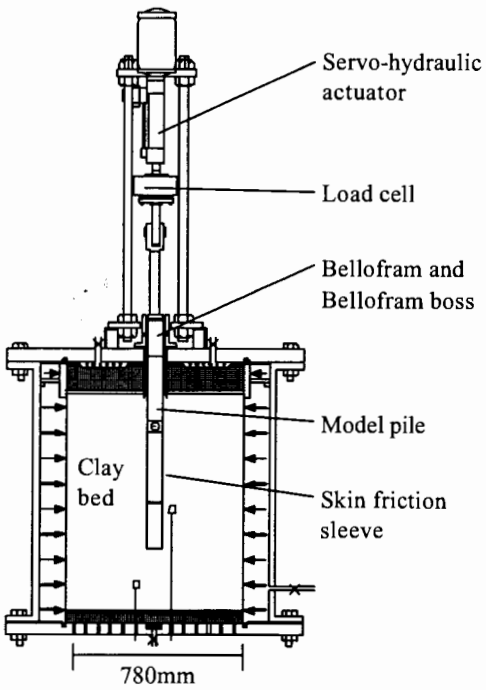

Fig. 9. Calibration chamber in pile testing mode

During Statnamic type pulse loading the PC mounted DAQ card was used to generate voltage representations (0 to 10 Volt DC) of the load pulses that were fed to the servo-hydraulic controller in load control mode. The generated load pulses were 180 ms duration and were designed to mimic the load profiles seen in prototype Statnamic tests.

Testing programme

Two types of model pile testing were undertaken. Firstly, constant rate penetration tests (CRP) were carried out at penetration rates varying from of 0.01 to 500 mm/s. To maximise the information from the clay bed the tests were carried out consecutively. After each individual test the load to the pile was removed and the clay sample allowed to re-consolidate. The re-consolidation was considered complete when the clay bed transducers showed pore water pressures close to the pre-drive values. Throughout the testing programme, CRP tests were undertaken at 0.01 mm/s to define a boundary for the low rate static pile capacity and allow for the effects of increased penetration and extended consolidation.

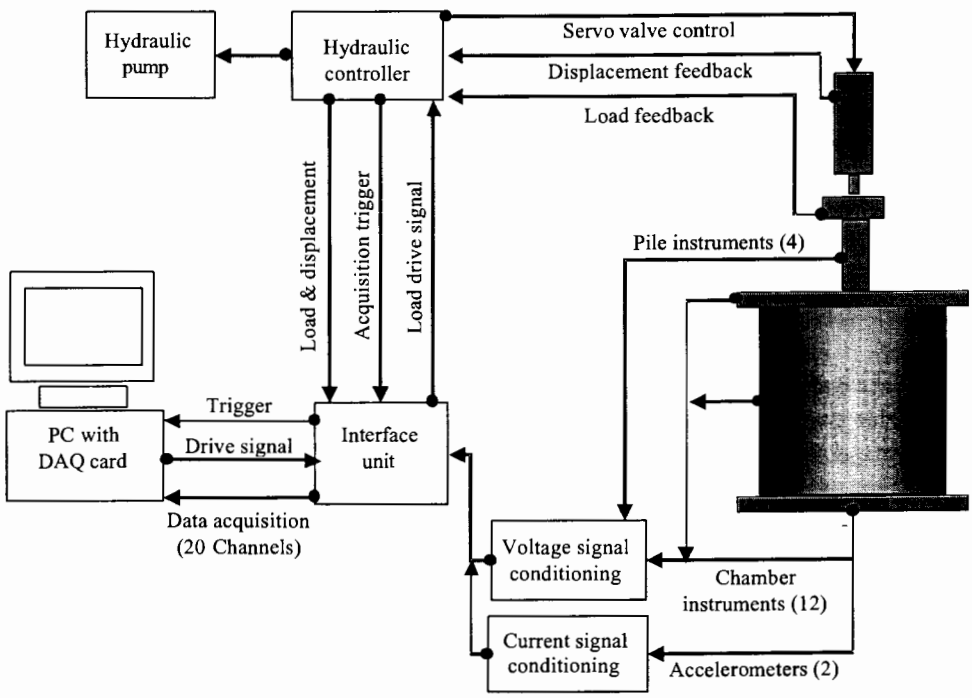

Fig. 10. Control and acquisition system

back signal during displacement-controlled tests. The actuator system was controlled by a digital servo-controller, which allowed closed loop control of the pile loading. A loading frame bolted to the chamber top end plate supported the actuator assembly. As the 150 mm long LVDT incorporated within the actuator was considered too insensitive, shorter stroke LVDTs (25 mm & 50 mm) independently measured the pile's displacement during load testing.

On completion of the constant rate of penetration test series the pile was subjected to load pulses similar to those recorded during field Statnamic testing. These pulses maintained the same load duration (≈ 180 ms) but with increased target loads of 10, 15, 20, 25 and 30 kN. A similar regime of re-consolidation was undertaken between each individual load pulse. The final Statnamic type pulse test was then followed by a CRP test at 0.01 mm/s for calibration purposes, as discussed above.

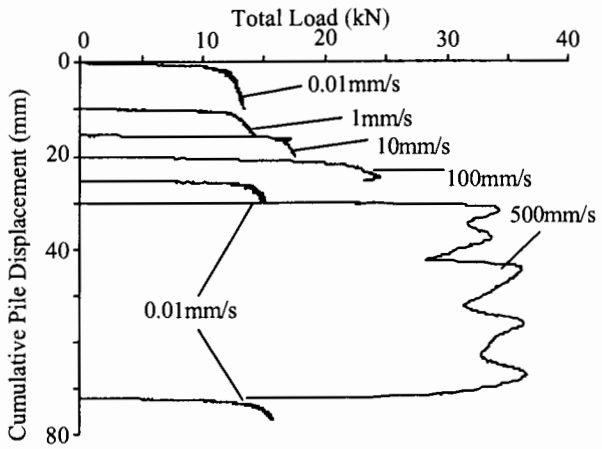

Fig. 11. Effect of pile penetration rate on total pile resistance during CRP tests

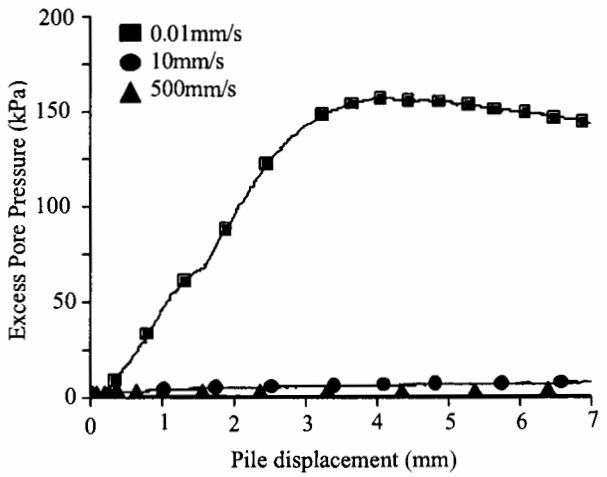

Fig. 12. Excess pore pressure at the pile tip during CRP tests at different rates

TEST RESULTS

Constant rate penetration tests

The effects of penetration rate on measured total pile resistance during the CRP tests can be seen in Fig. 11. Similar trends were also seen for the measured skin friction and pile tip resistance. For each test, the pile was driven a minimum of 7 mm (10% pile diameter), by which point it was assumed the ultimate load had been mobilized.

Positive excess pore water pressures of up to 150 kPa were generated at the pile tip during initial 0.01 mm/s tests within a clay bed. Subsequent 0.01 mm/s tests generated reduced maximum pore pressures probably due to overconsolidation of the clay below the pile tip. Excess pore pressures were recorded at the tip for both the 0.01 mm/s tests and reduced levels for the 10 mm/s tests (Fig. 12). No significant variation in pore pressure was noted during loading for tests carried out at rates above this. The excess pore water pressure generated at the pile shaft monitoring point during the 0.01 mm/s CRP tests displayed behaviour typical of over consolidation with positive excess pore water pressures indicating contraction followed very quickly by negative excess pore water pressures indicating dilation. Compared with the tip, the pressures generated were relatively small at ± 10 kPa, with little variation in magnitude between tests. Similar behaviour was noted at higher rates but the magnitude reducing with increasing rates made the variations much smaller at high rates.

Along with short term high rate logging during the tests, longer-term post test logging was normally undertaken (pile unloaded) at a reduced sampling rate. For the tests at 0.01 mm/s the tip pore pressure peaked at the end of loading (≈ 11 minutes) and then dissipated back to pre-test levels over a period of 16 hours. Conversely, skin readings increased to pre-test levels in approximately 4 minutes. For higher rate tests tip pore pressures rose to peak values of 32 to 47 kPa within 7 to 10 minutes after completing loading with similar dissipation back to pre-test levels.

The clay bed pore water pressure transducers were generally arrayed in sets of three at three different levels referred to as upper (246 to 309 mm), middle (508 to 536 mm) and lower (741 to 768 mm) where the distances are depths below the upper bed surface. The middle transducers were typically located in sets of three at radial distances of 57 mm, 92 mm and 127 mm (2.63 R, 3.63 R and 4.64 R, where R was the pile radius) from the pile surface. The pressures measured by the two transducers closest to the pile initially increased rapidly corresponding to the displacement at which the pile shaft capacity was fully mobilized (5 kPa), but then increased more gradually until the end of CRP at 0.01 mm/s (10 kPa). The outer transducer increased at a constant rate until reaching a similar pressure. For transducers located initially 41 mm in advance of the pile at radial distances of 33 mm (1.94 R) and 83 mm (3.60 R) from the pile center line, large positive excess pressures were generated with maximum values corresponding to maximum displacement. These were typically of the order of 170 kPa at 1.94 R and 70 kPa at 3.60 R.

For a penetration rate of 10 mm/s, the middle transducers measured small negative pressures (- 2 kPa) up to the point of maximum skin friction resistance, after which all the pressures tended to become positive and increased gradually towards the end of the test. At rates above 10 mm/s the behaviour was similar but with increasing negative (- 10 kPa) and positive pressures (20 kPa). The upper transducers displayed large negative values up to - 50 kPa at 500 mm/s. Results for middle transducers in a CRP test at 500 mm/s can be seen in Fig. 13a. Transducers

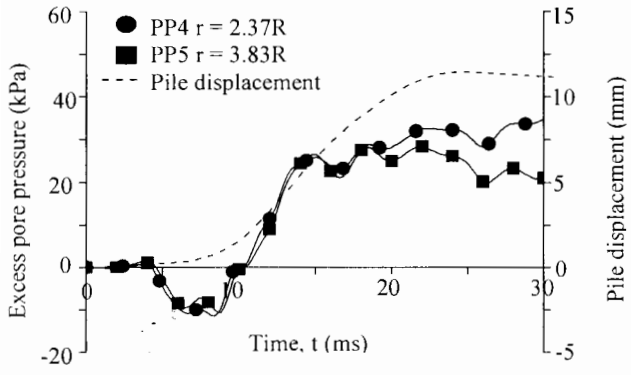

Fig. 13a. Excess pore pressure at bed mid-height during CRP at 500 mm/s. Pile displacement vs time Shown for reference

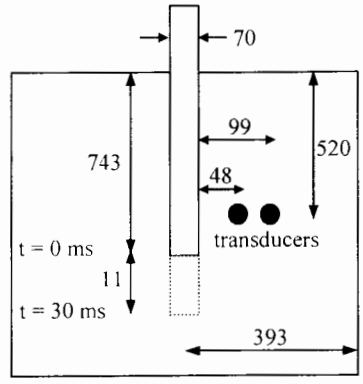

Fig. 13b. Relative positions of pile and pore pressure transducers during CRP at 500 mm/s. All dimensions in mm

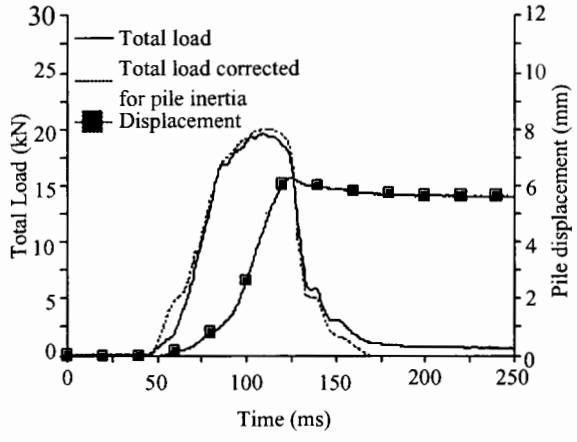

Fig. 14. Typical Statnamic test load pulse and resulting pile penetration

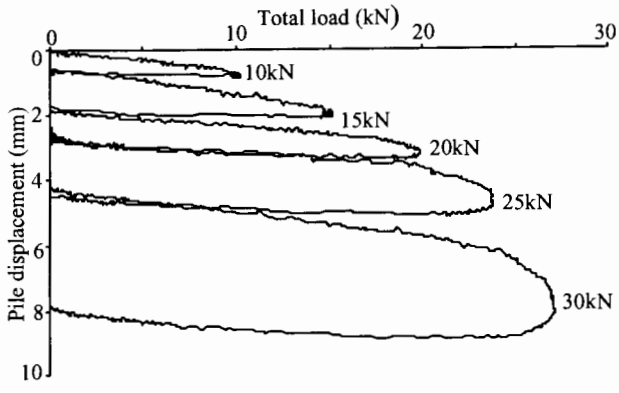

Fig. 15. Total applied load-displacement curve for Statnamic tests

located in front of the pile showed increased pressure response (265 kPa) for the transducer closest to the pile (radially) but initially negative (- 27 kPa) for the transducer located further away. As the test rate increased the pressure recorded by the closest transducer reduced to < 20 kPa whereas the outer unit indicated a negative pore pressures as low as - 100 kPa. There must be doubts about this pressure measurement because of possible cavitation even though every effort was made to maintain saturation. The bed pore pressure response close to the tip as well as being affected by pile penetration rate would also be influenced by the distance of the pile from the bed pore pressure measuring points.

Statnamic pulse load tests

A typical Statnamic type load pulse applied to the pile and the resulting displacements can be seen in Fig.14. This figure also shows the total load adjusted to allow for pile inertia. It can be seen that in the laboratory model the pile inertia component of the load is very small. The total applied load-displacement behaviour of the pile can be seen in Fig. 15. The load value labels on Fig. 15 correspond to the target load and not the maximum pile resistance achieved. It can be seen that as the STN target load increases the actual load reached is significantly lower as the pile reaches its STN ultimate capacity.

During the STN load tests no significant response was noted from the pile tip pore water pressure transducers. A very small increase in the skin pore pressure (+ 1 kPa) was noted with little variation in magnitude. This was then followed quickly by reduction to - 2 kPa on load removal. Long term monitoring of the tip results showed a gradual increase in pore pressure varying from 1.5 kPa for a 10 kN test to 27 kPa for a 30 kN test. Peak pore pressures were reached between 7 to 21 minutes after testing with dissipation back to pre-test levels over a period of 16 hours. The long term monitoring of the skin pore pressure showed a return to pre-test levels over 3 hours.

The upper array of clay bed transducers recorded increasing negative pore pressures throughout STN testing.

Maximum negative pressures (- 43 kPa) were recorded for the 30 kN tests with the pore pressures returning to pre-test levels on unloading. Very little change was noted in the unit located close to the pile with the variation increasing on moving away from the pile. Mid-height transducers increased rapidly up to 50 kPa for 30 kN STN with maximum pore pressure coinciding with the peak STN load. Again the higher pore pressures were noted further away from the pile. Positive pore pressures were noted in advance of the pile for all STN tests levels with maximum pore pressures of up to 210 kPa coinciding with peak STN load.

The response of the bed accelerometers was only monitored during the STN testing. Two accelerometers were maintained at fixed radial positions throughout the testing (3.37 R & 6.63 R) programme but their vertical heights were varied between beds. Measured peak bed accelerations increased with increasing STN peak load. The peak bed accelerations were found to reduce exponentially relative to the pile's acceleration with distance from the pile. Variation of the vertical position of the accelerometers revealed minimal bed accelerations near the pile tip level with a tendency to increase on moving up the pile shaft or moving below the tip.

DISCUSSION

Calibration chamber performance

Some problems were encountered with consolidometer membrane leakage during one-dimensional consolidation. As a consequence the changeover to triaxial consolidation varied from bed to bed. It was therefore essential to examine bed consistency after each series of tests to ensure that comparison of test results was valid.

During dismantling of the clay bed hand shear vane tests were carried out, and water content and undisturbed tube samples were taken, to check consistency within each bed and from bed to bed. Ignoring results from samples close to the pile position (< 4 R) where stress changes would have occurred in the clay during pile testing, there was a fair consistency both within beds and between beds. Water contents for the beds varied from 23.7% to 25.1% and the maximum standard deviation within any of the beds was 1.0 %. This is considered acceptable, particularly since it wasn't always practical to carry out the pile loading test at exactly 90% clay bed consolidation. Additionally, although good practice was used to minimise evaporation, the results from bed strip down may also have been influenced by drying as this operation normally took up to 2 days.

The hand shear vane testing gave a peak undrained shear strength of 53 kPa with a standard deviation of 5 kPa. Unconsolidated undrained triaxial tests carried out on 38 mm diameter specimens immediately after clay bed dismantling gave an average undrained strength of 56 kPa, although there was considerable scatter in the results as indicated by a standard deviation of 11 kPa. A limited number of consolidated undrained triaxial tests were carried out on 100 mm diameter specimens of KSS prepared from a slurry in a 100 mm diameter 1-D consolidation mould and then isotropically consolidated under a pressure of 250 kPa compared to the bed consolidation stress of 280 kPa in order to simulate the bed material when 90% consolidated. These gave an average undrained shear strength of 75 kPa. This is somewhat higher than the unconsolidated undrained test strengths from specimens obtained from the clay bed after pile testing and is almost certainly due to stress relief and sampling disturbance during chamber dismantling as well as the different sample sizes and methods of preparation.

Figure 11 includes the results of 3 CRP tests with penetration rates of 0.01 mm/s carried out as part of the multi-stage testing with reconsolidation procedure. The similarity in the load-displacement curves confirms the acceptability of using this procedure.

Analysis of the test results after testing revealed that considerable variation was occurring in both vertical and horizontal confining pressures during all tests above 0.01mm/s (CRP) as shown in Fig. 16. The variation took the form of a reduction of up to 52 kPa in top cell pressure for the majority of the pile penetration. The side pressure system reduced initially by up to 15 kPa followed by a positive increase part way through penetration. In most cases the lowest pressures were associated with the peak load applied to the pile. It is assumed that these variations were caused by upward movement of the chamber top plate which was used as a reaction for the pile load. As the load application was very rapid the chamber's pressure supply system could not accommodate the resulting rapid change in pressure. This limits the interpretation of the bed pore pressure transducer results. The minimisation of deformation and improvement of the response of the cell pressure system requires further investigation.

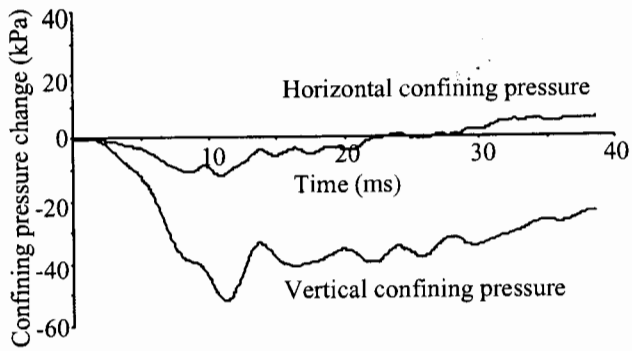

Fig. 16. Variation in bed confining pressure during CRP at 500 mm/s

Model pile and loading system performance

O-ring seals were used throughout the pile and in particular at the seals for movement of the pile tip and skin friction sleeves. It is acknowledged that these seals may give variable resistance to movement and their behaviour may vary with the varying rate of pile testing. The effect of this was not assessed due to the high velocities involved, which in turn were associated with very small movements of the measuring devices, but it is considered that any variation will have a negligible effect on the test data.

The performance of the hydraulic loading system was limited by the size and weight (18.9 kg) of the model pile. This resulted in pile velocity variations for CRP testing in the working range of the pile's capacity. The ultimate load was defined at a penetration equivalent to 10% of the pile diameter because by this stage the pile's velocity had been constant for several millimetres. This velocity variation limits the validity of commenting on the influence of penetration rate in the zone of elastic pile response. The values of velocity quoted for CRP tests refer to the target velocity rather than that actually achieved. The velocities used for analysis of the rate effects were taken as the average velocity up to the point of penetration equivalent to 10% pile diameter.

The use of a hydraulic loading system proved challenging for such high rate testing as the system gain had to be tuned to suit each test rate or loading type. Due to the long time periods associated with clay bed preparation and test construction this resulted in tuning taking place throughout testing. Unlike a prototype pile loading system the actuator needed to be rigidly connected to the pile to maintain system stiffness. This meant that great care had to be taken during pile connection and high speed unloading not to load the pile in tension or compression before or after testing.

CRP testing

The load capacity of the pile was found to be particularly sensitive to pile penetration rate, with significant increases in pile capacity between the rates of 10 to 500 mm/s. This effect was more pronounced for the skin friction component of the pile capacity than the pile tip. A similar response was noted by Dayal and Allen (1975), who found that the friction on a penetrometer driven into a clay target suddenly increased at 15 mm/s. To aid comparison of the results the loading rate effect for the various components of pile resistance are shown in Fig. 17. Here pile capacity (R_d) at speeds above the static capacity (R_s) determined at 0.01 mm/s has been plotted against penetration rate. From Fig. 17, it is apparent that the loading rate effect on a pile in fine grained soils is not a linear relationship but more closely follows a power law (Equation 1) as suggested by Gibson and Coyle (1968).

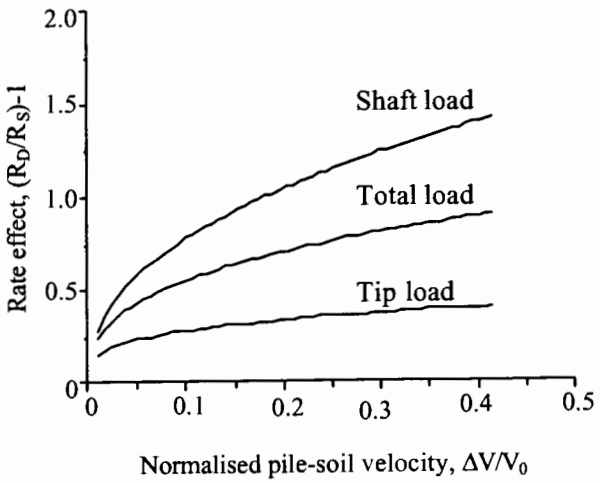

Fig. 17. Rate effects for the various componemts of pile capacity

$$\frac{R_d}{R_s} = 1 + JV^N \tag{1}$$

where J = a viscous soil damping constant; and V = velocity of pile penetration.

This relationship was modified by Randolph and Deeks (1992) to describe the viscous rate dependency of a piles shaft capacity during plastic deformation (Equation 2).

$$\frac{\tau_d}{\tau_s} = \left[1 + \alpha \left(\frac{V}{V_o} \right)^{\beta} \right] \tag{2}$$

where α and β are damping constants and V_o is a reference velocity of 1 m/s.

The values of the damping parameters for shaft resistance in the KSS material were found to be $\alpha = 2$ and $\beta = 0.4$ but considerable scatter was experienced in the data giving 95% confidence limits of $\alpha = 1.5$ to 2.7 and $\beta = 0.2$ to 0.6. The application of the power law based rate effect was suitable for the total measured pile resistance and the shaft resistance but it does not adequately describe the lower capacity enhancement seen at the pile tip.

As the 0.01 mm/s CRP testing in a bed progressed a reduction in the pile interface pore pressure response was noticed. This is attributed to the change in degree of bed consolidation. As mentioned above the moisture contents measured for the bed on strip down were particularly consistent from 4 R outwards. Closer to the pile considerable variation in the moisture content was noted especially at the tip, with values 4.5 to 6.5% lower up to 20 mm below the tip. In the pile skin region the variation was typically 1.5 to 2.5% less but little variation was noted after 3.5 to 4 R.

The pore pressure response of the bed was also affected by the rate of pile penetration. For the upper and mid-height transducers it is difficult to separate the effect of the variation of the confining pressure due to chamber deformation. This reduction in confining pressure does not appear to have had a major influence on the rate effects although it may explain some of the scatter in the results. For future studies the chamber top will be stiffened by the addition of structural units tensioned against identical units running below the chamber base plate. Remote deflection monitoring of the chamber top plate will also be undertaken.

Statnamic testing

For STN loading there was minimal permanent displacement of the pile until the 20 kN pulse load where the maximum load applied was 18.3 kN corresponding to a low rate CRP capacity of 14.2 kN. Comparison of Statnamic pulses (STN) with CRP tests at 0.01 mm/s shows that the stiffness response of the pile is very similar to the CRP test at small penetrations (Fig. 18). The increased stiffness during the STN test is then apparent as the low rate capacity moves from elastic to plastic type behaviour. This suggests that for the initial elastic portion of an STN test, the capacity is independent of pile penetration rate and that the reductions for viscous damping are not valid until the STN pile capacity approaches low rate ultimate capacity or plastic behaviour. The results presented in Fig. 15 show that pile capacity increased with increasing STN target load. This is due to the increase in pile velocity with increasing target load.

The lack of response for pile pore pressure transducers during the actual short duration testing highlights the need for long term low rate logging after a high speed event in a fine grained soil. The Kulite pore pressure transducers were tested in their mountings for response and were found to have 99% response to a step load of 300 kPa applied over a range of 10 ms to 100 ms. The response in the clay depends on the degree of saturation, permeability and compressibility of the soil. Bond et al. (1991) calculated for their model pile that 3 seconds were required for the systems to register 95% of the true pore pressure in London Clay. The impact of using silicon oil as the saturation fluid was investigated by Lee (1990) for a similar transducer arrangement and he showed that a loss of only 5% of applied pressure for a pressure fluctuation of 1 kHz would occur for a liquid 20 (20 W) times more viscous than water. The phase lag for a fluid of 50 W was reported as 26° increasing to 56° for a transducer at 50% saturation, highlighting the need for careful saturation during rapid testing.

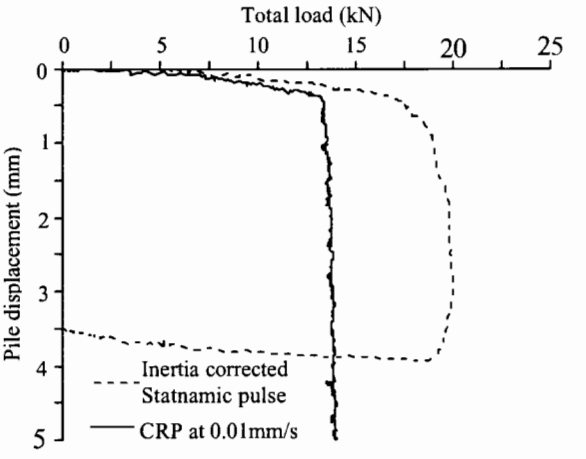

Fig. 18. Comparison of pile load-displacment behaviour during Statnamic and CRP testing

Given the limited number of accelerometers used for this study it is difficult to draw any direct conclusions. Additional accelerometers will be incorporated in a further study with up to eight units incorporated in the bed. Units will also be oriented horizontally to enhance understanding of soil accelerations throughout the bed.

CONCLUSIONS

1. A clay calibration chamber can be used to create uniform and repeatable clay beds suitable for carrying out parametric studies using an instrumented model pile. However, it should be recognized that load testing at very high rates raises challenges not found at lower rates.
2. The validity of carrying out multiple tests in the same bed with reconsolidation between tests has been demonstrated.
3. As rate of pile penetration increases during the CRP test the pile capacity also increases. This is especially true for the skin friction component at penetration rates above 10 mm/s.
4. The rate effect adequately fits a power law relationship as suggested by Gibson & Coyle (1968) for the total pile resistance and the shaft resistance. Although, the pile's tip resistance shows an enhancement with increasing penetration rate it does not fit a power law relationship.
5. During Statnamic pulse type loads the pile load capacity and velocity increases as the Statnamic target load increases.
6. Results of bed pore pressure monitoring during low rate CRP testing indicated behaviour corresponding to increasing over consolidation with each additional test performed.

ACKNOWLEDGEMENT

This research project has been supported by EPSRC (Grant No. GR/M64017/01) with the assistance of Berminghammer Foundation Equipment (Canada), TNO Building Research (Netherlands), The Expanded Piling Company (UK) and Precision Monitoring and Control (UK). Thanks are also extended to Juan Balderas-Meca for provision of results from element testing of the KSS material.

REFERENCES

1) Anderson, W.F., Pyrah, I.C. and Fryer, S.J. (1991): "A clay calibration chamber for testing field devices," ASTM Geotechnical Testing Journal 14, No. 4, pp. 440-450.
2) Balderas-Meca, J. (2004): "Rate effects in rapid loading of clay soils," PhD Thesis, University of Sheffield, UK. (in preparation).
3) Bell, F.G. (1987): "Ground Engineer's Reference Book," 1st ed., Butterworth & Co., London, pp. 58/3-58/13.
4) Bermingham, P.A., Ealy, C.D. and White, J.K. (1994): "A comparison of Statnamic and static field tests at seven FHWA sites," Proc. HTE. Int. Conf. on Design & Construction of Deep Foundations, pp. 616-630.
5) Bond, A.J., Jardine, R.J. and Dalton, J.C.P. (1991): "Design and performance of the Imperial College instrumented pile," ASTM Geotechnical Testing Journal 14, No. 4, pp. 413-424.
6) Brown, D.A. (1994): "Evaluation of static capacity of deep foundations from Statnamic testing," ASTM Geotechnical Testing Journal 17, No. 4, pp. 403-414.
7) Casagrande, A. and Shannon, W.L. (1948): "Stress deformation and strength characteristics of soils under dynamic loads," Proc. 5th Int. Conf. on Soil Mechanics and Foundation Engineering, pp. 29-34.
8) Dayal, U. and Allen, J.H. (1975): "The effect of penetration rate on the strength of remoulded clay and sand samples," Canadian Geotechnical Journal 12, pp. 336-348.
9) Department Of Energy (1990): "Research on the behaviour of displacement piles in an overconsolidated clay," Dept. of Energy (DOE)-Offshore Technology Report OTH 89 296, Imperial College, London, HMSO Publications Centre, London, 34p.
10) Eid, M. M. (1978): "Expansion of cylindrical cavities in clay," PhD Thesis, University of Sheffield, UK.
11) Gibson, G.C. and Coyle, H.M. (1968): "Soil damping constants related to common soil properties in sands and clays (Bearing Capacity for Axially Loaded Piles)." Texas Transportation Institute Research Report 125-1 (Study 2-5-67-125),Texas A&M University.
12) Hyde, A.F.L., Robinson, S.A. and Anderson W.F. (1998): "Rate effects in clay soils and their relevance to Statnamic pile testing," Proc. 2nd Int. Statnamic Seminar, Tokyo, Japan, pp. 303-309.
13) Kusakabe, O. and Matsumoto, T. (1995): "Statnamic tests of Shonan test program with review of signal interpretation," Proc. 1st Int. Statnamic Seminar, Vancouver, Canada, pp. 113-122.
14) Lee, F.K. (1990): "Frequency response of diaphragm pore pressure transducers in dynamic centrifuge model tests." ASTM Geotechnical Testing Journal 13, No. 3, pp. 201-207.
15) McManus, K.J. and Kulhawy, F.H. (1991): "A cohesive soil for large-size laboratory deposits," ASTM Geotechnical Testing Journal 14, No. 1, pp. 26-34.
16) Middendorp, P. (1993): "First experiences with Statnamic load testing of foundation piles in Europe," Proc. Deep Foundations on Bored and Auger Piles, pp. 265-272.
17) Randolph, M.F. and Deeks, A.J. (1992): "Dynamic and static soil models for axial pile response," Proc. 4th Int. Conf. on the Application of Stress Wave Theory to Piles, The Hague, Netherlands, pp. 3-14.
18) Rossato, G., Ninis, N.L. and Jardine, R.J. (1992): "Properties of some kaolin-based model clay soils," ASTM Geotechnical Testing Journal 15, No. 2, pp. 166-179.
19) Sheeran, D. and Krizeck, R.J. (1971): "Preparation of homogeneous soil samples by slurry consolidation," Journal of Materials 6, No. 2, pp. 356-373.
20) Smith, M. G. (1993): "A laboratory study of the Marchetti Dilatometer." PhD Thesis, University of Oxford, UK.
21) Taylor, R.N. (1995): "Geotechnical Centrifuge Technology," 1st ed., Blackie Academic and Professional, Glasgow.